

Detecting Hidden Synchronization Between Chaotic Signals: A Kernel-based Approach

Hiromichi Suetani¹, Yukito Iba², and Kazuyuki Aihara^{3,1}

¹*Aihara Complexity Modelling Project, ERATO, JST, Uehara, Shibuya-ku, Tokyo 151-0064, Japan*

²*The Institute of Statistical Mathematics, Minami-Azabu, Minato-ku, Tokyo 106-8569, Japan and*

³*Institute of Industrial Science, The University of Tokyo, Komaba, Meguro-ku, Tokyo 153-8505, Japan*

(Dated: November 13, 2018)

A unified framework for analyzing generalized synchronization in coupled chaotic systems from data is proposed. The key of the proposed approach is the use of the *kernel methods* recently developed in the field of machine learning. Several successful applications are presented, which show the capability of the kernel-based approach for detecting generalized synchronization. It is also shown that the dynamical change of the coupling coefficient between two chaotic systems can be captured by the proposed approach.

PACS numbers: 05.45.Xt, 05.45.Tp, 02.50.Sk, 05.10.-a

Synchronization of chaotic systems has been an active research area in recent years [1]. Now the notion of synchronization of chaotic systems is extended far beyond complete synchronization between identical systems [2], and various kinds of nonlinear synchronization have been proposed in the literature [1]. Among them, a most general form is *generalized synchronization (GS)* [3]. GS is said to occur if there exists a time-independent nonlinear functional relationship $y = \Psi(x)$ between the states x and y of two systems X and Y .

Experimental detection and characterization of GS from observed data is a challenging problem, especially from the viewpoint of applications in biology. It is useful for the study on the nonlinear interdependencies observed in binding of different features in cognitive process [4] and epilepsies in the brain [5].

In unidirectionally coupled systems, a way to detect GS is to make an identical copy Y' of the response system Y driven by the common signal from the driver system X , then investigate whether orbits of both Y and Y' coincide after transient [6]. However, it is very difficult to prepare a complete identical copy of the response system, and this approach does not give any information on the structure of the synchronization manifold $\mathcal{M} = \{(x, y) : y = \Psi(x)\}$ in the state space.

On the other hand, several indices have been proposed in Refs. [3, 5, 7, 8], quantifying the nonlinear dependence between X and Y based on local linear relationships between them. While the usefulness of these indices were shown in some examples [5, 7], those approaches are still ad-hoc, lacking systematic methods for unifying local linear relationships of different regions in the state space.

In this Letter, we propose a novel framework for analyzing GS. The proposed approach is based on *Kernel Canonical Correlation Analysis (Kernel CCA)* [9, 10], which is a version of *kernel methods* that have been attracting much attention in the machine learning community [10, 11, 12]. We will demonstrate its capability for treating GS with several successful applications. The

proposed method does not require explicit knowledge on the underlying equation behind time series. Although we restrict our attention to the analysis of numerical experiments here, it is also applicable to experimental data.

Canonical Correlation Analysis (CCA), a linear version of Kernel CCA, is a multivariate analysis method to find a pair of vectors that maximize the correlation coefficient between projections of signals onto them [13]. CCA is useful for detecting a linear relationship between a pair of multidimensional data sets, but cannot deal with the case like GS where nonlinearity is essential. Extending the ability of CCA for analyzing data with nonlinearity, kernelization of CCA has been proposed by several researchers [9, 10]. An intuitive formulation of Kernel CCA is as follows.

For a given data set $\{(x_n, y_n)\}_{n=1}^N$, $x_n \in \mathbb{R}^p$ and $y_n \in \mathbb{R}^q$, Kernel CCA seeks a pair of nonlinear scalar functions $f : \mathbb{R}^p \rightarrow \mathbb{R}$ and $g : \mathbb{R}^q \rightarrow \mathbb{R}$ such that an estimator of the correlation coefficient

$$\rho_{\mathcal{F}} = \frac{\text{cov}(f(x), g(y))}{\sqrt{\text{var}(f(x))} \sqrt{\text{var}(g(y))}} \quad (1)$$

between $f(x)$ and $g(y)$ is maximized.

The essence of the kernel methods is an assumption that nonlinear functions f and g are well approximated by linear combinations of *kernels* on data points (x_i, y_i) : $f(\cdot) = \sum_{i=1}^N \alpha_i k(x_i, \cdot)$ and $g(\cdot) = \sum_{i=1}^N \beta_i k(y_i, \cdot)$. Examples of kernels are $k(x, x') = \exp(-\|x - x'\|^2 / 2\sigma^2)$ (Gaussian), $((x \cdot x') + \theta)^d$ (Polynomial), $\tanh(\eta(x \cdot x') + \theta)$ (Sigmoidal) [10, 11, 12]. A rich representation of nonlinear functions is allowed by suitably chosen weight coefficients $\alpha = \{\alpha_i\}$, $\beta = \{\beta_i\}$ and kernel parameters. At first sight, the dependence of the expressions for f and g on given data $\{(x_n, y_n)\}_{n=1}^N$ brings some ad-hoc nature to the method. The assumption is, however, equivalent to the assumption that the functions f and g belong to a Reproducing Kernel Hilbert Space (RKHS), and sound mathematical foundation is provided by the theory of RKHS [10, 11, 12].

Substituting the expressions for f and g into Eq. (1), and replacing covariance $\text{cov}(\cdot, \cdot)$ and variances $\text{var}(\cdot)$ with empirical averages over the data set $\{(x_n, y_n)\}_{n=1}^N$, Kernel CCA reduces to the maximization of

$$\rho_{\mathcal{F}} = \frac{t\alpha K_X K_Y \beta}{\sqrt{t\alpha K_X^2 \alpha + \kappa \|\mathbf{w}_X\|^2} \sqrt{t\beta K_Y^2 \beta + \kappa \|\mathbf{w}_Y\|^2}}, \quad (2)$$

where K_X, K_Y are the *Gram matrices* $(K_X)_{i,j} = k(x_i, x_j)$ and $(K_Y)_{i,j} = k(y_i, y_j)$ defined with given data. Here, the terms $\|\mathbf{w}_X\|^2 = \sum_{n=1}^N \alpha_n f(x_n) = \alpha' K_X \alpha$, $\|\mathbf{w}_Y\|^2 = \sum_{n=1}^N \beta_n g(y_n) = \beta' K_Y \beta$ are introduced in order to avoid over-fitting. Although the parameter $\kappa \neq 0$ is required for a nontrivial result, the precise value of κ is not important [14]. For simplicity, we tentatively assume that the averages of $\{f(x_n)\}_{n=1}^N$ and $\{g(y_n)\}_{n=1}^N$ are zero. Later we will show that subtraction of the averages from data can be done in a clever way and does not cause any technical difficulty.

The maximization of Eq. (2) leads to the following generalized eigenvalue problem [9]:

$$\begin{pmatrix} 0 & K_X K_Y \\ K_Y K_X & 0 \end{pmatrix} \begin{pmatrix} \alpha \\ \beta \end{pmatrix} = \rho \begin{pmatrix} K_X(K_X + \kappa I) & 0 \\ 0 & K_Y(K_Y + \kappa I) \end{pmatrix} \begin{pmatrix} \alpha \\ \beta \end{pmatrix}. \quad (3)$$

The first eigenvalue of Eq. (3) gives the maximal value $\rho_{\mathcal{F}}^{\max}$ of $\rho_{\mathcal{F}}$ in Eq. (1). The index $\rho_{\mathcal{F}}^{\max}$ is called the *canonical correlation coefficient*, and the variables $u = f(x)$ and $v = g(y)$ transformed by f and g are called *canonical variates* of Kernel CCA, respectively.

So far, the averages of $\{f(x_n)\}_{n=1}^N$ and $\{g(y_n)\}_{n=1}^N$ are set to zero. In fact, it is not necessary to subtract the averages explicitly, because the subtraction of the means is equivalent to the replacement of the Gram matrices K in Eq. (3) with $\tilde{K} = K - (1/N)(\mathbf{j} \mathbf{j}^t)K - (1/N)K(\mathbf{j} \mathbf{j}^t) + (1/N^2)(\mathbf{j} \mathbf{j}^t)K(\mathbf{j} \mathbf{j}^t)$, where \mathbf{j} is a N -dimensional vector such that each component equals to the unity [10, 11, 12].

Let us start with an example of the unidirectionally coupled Hénon maps with equations

$$X : \begin{cases} x'_1 = 1.4 - x_1^2 + 0.3x_2 \\ x'_2 = x_1, \end{cases} \quad (4)$$

$$Y : \begin{cases} y'_1 = 1.4 - \{\gamma x_1 y_1 + (1 - \gamma)y_1^2\} + 0.1y_2 \\ y'_2 = y_1, \end{cases} \quad (5)$$

where γ denotes the coupling coefficient between two systems X and Y . Figures 1 (a) and (b) show the projections of the strange attractors of the system Eqs. (4) and (5) with $\gamma = 0.0$ and 0.25 onto the (x_1, y_1) plane, respectively. When the coupling is strong, the complicated driver-response relation with strong nonlinearity is formed between two different chaotic dynamics. It can be identified in Fig. 1 (b) with a visual inspection, but it is not easy to represent it by naive mathematical tools such as correlation coefficients.

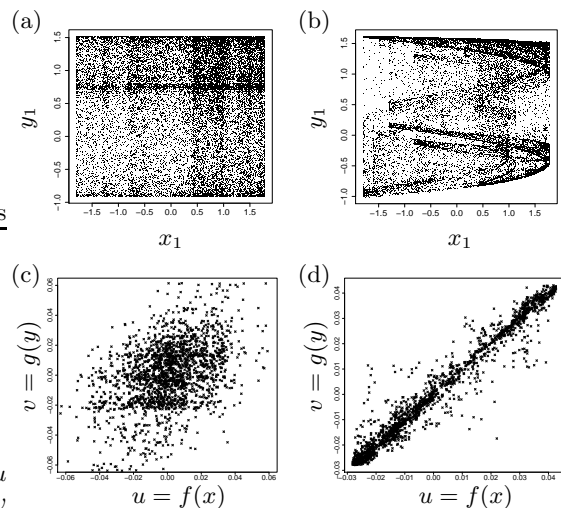


FIG. 1: (a, b) Projections of strange attractors of the coupled Hénon maps onto the (x_1, y_1) plane, $\gamma = 0.0$ in (a) and $\gamma = 0.25$ in (b). (c, d) Scatter plots of the canonical variates of Kernel CCA, $\gamma = 0.0$ in (c) and $\gamma = 0.25$ in (d).

Then, we apply Kernel CCA to these cases. Here, we employ a Gaussian kernel with $\sigma = 0.1$ and κ is set to 0.3 . We prepare an orbit with length $N = 2 \times 10^3$ as training data and each of variables x_1, x_2, y_1 , and y_2 is normalized within the unit interval $[0, 1]$. Figures 1 (c) and (d) illustrate results of Kernel CCA. Figure 1 (d) shows that GS is clearly identified as a cloud of points along the diagonal on the plane of the canonical variates. On the other hand, when X and Y are independent, the correlation between the canonical variates is very weak, which indicates that Kernel CCA does not detect spurious synchronization (Fig. 1 (c)).

We also investigate the dependence of the canonical correlation coefficient $\rho_{\mathcal{F}}^{\max}$ on the coupling coefficient γ . Figure 2 indicates the rapid increase of $\rho_{\mathcal{F}}^{\max}$ against γ in an interval $0 < \gamma < 0.17$. In Inset (i) of Fig. 2, the maximal Lyapunov exponent λ_R of the response system Y is plotted as a function of γ . The exponent λ_R decreases with the increase of γ and becomes negative at $\gamma \sim 0.17$. In unidirectionally coupled systems, a necessary condition for the occurrence of GS is $\lambda_R < 0$ [6]. Therefore, the rapid increase of $\rho_{\mathcal{F}}^{\max}$ shown in the graph of $\rho_{\mathcal{F}}^{\max}$ vs. γ is consistent with the rapid decrease of λ_R shown in that of λ_R vs. γ . Moreover, there exists an interval where the value of $\rho_{\mathcal{F}}^{\max}$ changes nonmonotonically against γ as shown in Inset (ii) of Fig. 2. Such nonmonotonic change is also observed in the graph of λ vs. γ . These results tell us that $\rho_{\mathcal{F}}^{\max}$ can characterize subtle change as well as global tendency of GS.

The canonical correlation coefficient of the linear CCA as a function of γ is also plotted in Fig. 2, which shows that CCA cannot capture nonlinear dependencies in the

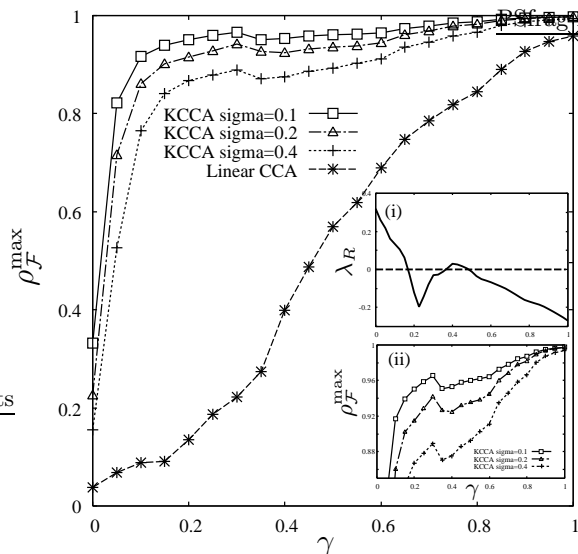


FIG. 2: The canonical correlation coefficient $\rho_{\mathcal{F}}^{\max}$ of Kernel CCA as a function of γ for three different values of σ , $\kappa = 0.1$ and $N = 10^3$. Inset (i): The maximal Lyapunov exponent λ_R of the response system vs. γ . Inset (ii): An enlargement of the graph of $\rho_{\mathcal{F}}^{\max}$ vs. γ .

system.

Next, in order to illustrate the capability of Kernel CCA in more complicated situations, we refer to the following FitzHugh-Nagumo neuron model modulated by chaotic dynamics of the Rössler model [15]:

$$X : \begin{cases} \dot{x}_1 = -\omega(x_2 + x_3) \\ \dot{x}_2 = \omega(x_1 + 0.36x_2) \\ \dot{x}_3 = \omega(0.4 + x_3(x_1 - 4.5)), \end{cases} \quad (6)$$

$$Y : \begin{cases} 0.02 \cdot \dot{y}_1 = -y_1(y_1 - 0.5)(y_1 - 1) - y_2 + S(t) \\ \dot{y}_2 = y_1 - y_2 - 0.15, \end{cases} \quad (7)$$

where the term $S(t) = 0.23 + 0.0075x_1(t)$ defines a chaotic inputs to the neuron, and ω is a parameter that controls the dominant time scale of the Rössler dynamics. We investigate the relation between the input chaotic stimulus and the output interspike intervals (ISIs) from the viewpoint of GS.

We define the i -th ISI as $s_i = t_i - t_{i-1}$ where t_i is onset time of the i -th spike when the variable y_1 makes upward crossing over some fixed threshold (set to 0.7 here). We also define the chaotic stimulus associated with the i -th ISI as $r_i \equiv x_1(t_i)$, which is the value of x_1 in Eq. (6) at t_i . By using the delay embedding scheme, we transform the time series $\{r_i\}$ and $\{s_i\}$ into the points $\{(r_i, r_{i-1}, \dots, r_{i-d_X+1})\}$ and $\{(s_i, s_{i-1}, \dots, s_{i-d_Y+1})\}$ in d_X and d_Y -dimensional state spaces, respectively. We set $d_X = d_Y = 3$ here and apply Kernel CCA to these data sets.

In Fig. 3 (a), significant nonlinear dependence between the input chaos and the output ISI is observed in a scatter

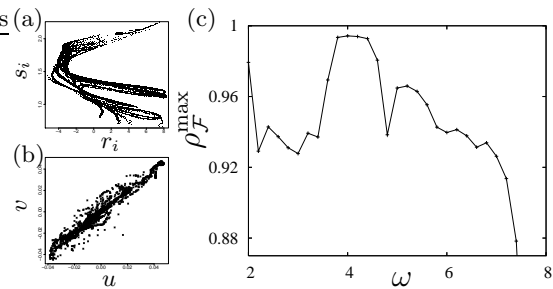


FIG. 3: (a) Scatter plots of r_i and s_i , and (b) scatter plot of u and v of the system Eqs. (6) and (7) with $\omega = 3.4$. (c) The canonical correlation coefficient $\rho_{\mathcal{F}}^{\max}$ of Kernel CCA as a function of ω , $\sigma = 0.5$, $\kappa = 0.1$, and $N = 2 \times 10^3$.

plot of (r_i, s_i) . Again, it is difficult to represent and detect such a complicated relation. Figure 3 (b) shows a scatter plot of the canonical variates of Kernel CCA associated with Fig. 3 (a). In this plot, it is easy to see that the canonical variates u and v are strongly correlated each other, which indicates that the system is in the state of GS.

The relation between r_i and s_i changes according to the value of the control parameter ω . In Fig. 3 (c), the canonical correlation coefficient $\rho_{\mathcal{F}}^{\max}$ is plotted as a function of ω , which visualizes the change of the input-output relation between two systems Eqs. (6) and (7). The index $\rho_{\mathcal{F}}^{\max}$ changes nonmonotonically with the increase of ω , and there is a regime around $\omega \sim 4$ where the value of $\rho_{\mathcal{F}}^{\max}$ is large. In addition to GS, chaotic phase synchronization (CPS) [16] occurs between two systems in this regime [15]. The increase of $\rho_{\mathcal{F}}^{\max}$ in this regime can be attributed to the occurrence of CPS.

So far, we have focused on the first eigenvalue $\rho_{\mathcal{F}}^{\max}$. We turn our attention to the eigenvector ${}^t(\alpha, \beta)$ in Eq. (3) and investigate changes of the structure of the dynamical system with Kernel CCA.

As an illustration, let us consider a problem of extracting nonstationary changes of the coupling coefficient γ from time series data of the coupled Hénon maps. An example of such changes are shown in Fig. 4 (b). When the value of γ varies from γ_0 , an orbit leaves from the synchronization manifold \mathcal{M} with γ_0 , and is attracted again to it when the value of γ is restored to γ_0 . As shown in Fig. 4 (a), the time series of the original variables (x_1, y_1) does not tell us whether the orbit is lying on \mathcal{M} or not at a given time t . By using Kernel CCA, a deviation of the orbit from \mathcal{M} will be detected as a large value of $|f(x) - g(y)|$, where $f(\cdot)$ and $g(\cdot)$ are nonlinear transformations determined by the first eigenvector ${}^t(\alpha, \beta)$.

Numerical experiments are performed with $\gamma_0 = 0.6$ in two different conditions, and results are shown in Figs. 4 (c) and (d), respectively. Figure 4 (c) shows the case where $f(\cdot)$ and $g(\cdot)$ are estimated from an orbit with

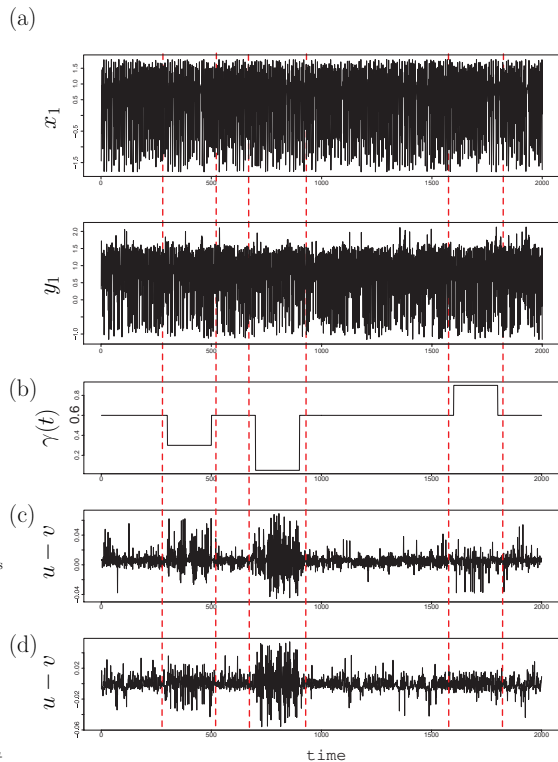


FIG. 4: (a) Time series of the variables x_1 and y_1 of the coupled Hénon maps when the value of γ changes temporally as shown in (b). (c, d) Time series of the difference of the canonical variates of Kernel CCA, $\sigma = 0.1$ and $\kappa = 0.1$ in (c), and $\sigma = 0.2$ and $\kappa = 0.1$ in (d).

$\gamma = \gamma_0$, which is prepared separately from the orbit to be analyzed. In Fig. 4 (c), time intervals where the values of γ are different from γ_0 is clearly detected as successive bursts in the time series of $|f(x) - g(y)|$.

In Fig. 4 (d), we show the case where the orbit to be analyzed is also used for estimating $f(\cdot)$ and $g(\cdot)$. We see that even when estimation of nonlinear transformations is affected by “noise” from the points not lying on \mathcal{M} , successive bursts are still observed in the time series of $|f(x) - g(y)|$ except for the one in a time interval $1600 \leq t < 1800$.

Finally, we mention how the parameters of Kernel CCA such as the width σ of a Gaussian kernel can be chosen according to a given data set. In order to represent complicated nonlinear structures via linear combinations of Gaussian kernels, the value of σ should not be too large. On the other hand, if σ is set to a too small value, the result is over-fitted to a given data, which may lead to a spurious detection of GS.

A way to overcome this problem is *cross-validation* (CV) [17]. In CV, a portion of sample data is set aside as “testing” data leaving the remainder as “training” data. Then, after learning is done by using the training data, the performance of the estimated model on new data is

validated by the testing data. Our preliminary experiments show that a method based on CV gives promising results in optimizing the parameter σ . The results will be published elsewhere [18].

In summary, we have proposed a new approach for analyzing GS in a unified framework of a kernel method. We have tested the proposed approach by applying it to several examples exhibiting GS, and demonstrated that the canonical correlation coefficient of Kernel CCA is a suitable index for the characterization of GS. In addition, it is shown that nonstationary changes of the coupling are detected from the time series by the difference between canonical variates of Kernel CCA.

The approach based on Kernel CCA provides not only an index for measuring nonlinear interdependence but also global nonlinear coordinates that enable us to reveal nonlinear dynamics hidden in data. In this respect, it goes beyond conventional methods of analyzing GS. Our attempts open the possibility of the kernel methods for analyzing complex dynamics observed in nonlinear systems.

We thank S. Akaho for stimulating discussions on the kernel methods. We are also grateful to K. Fukumizu for useful comments and informing us results on prior to publication.

-
- [1] A. Pikovsky, M. Rosenblum, and J. Kurths, *Synchronization, A Universal Concept in Nonlinear Sciences*(Cambridge University Press, Cambridge, 2001).
 - [2] H. Fujisaka and T. Yamada, Prog. Theor. Phys. **69**, 32 (1983); A.S. Pikovsky, Z. Phys. B: Cond. Mat. **55**, 149 (1984); L.M. Pecora and T.L. Carroll, Phys. Rev. Lett. **64**, 821 (1990).
 - [3] N.F. Rulkov, M.M. Sushchik, L.S. Tsimring, and H.D.I. Abarbanel, Phys. Rev. E **51**, 980 (1995).
 - [4] S.F. Farmer, J. Physiology **509**, 3(1998).
 - [5] M. Le Van Quyen et al., Physica D **127**, 250 (1999); J. Arnhold et al., Physica D **134**, 419 (1999).
 - [6] L. Kocarev and U. Parlitz, Phys. Rev. Lett. **76**, 1816 (1996); H.D.I. Abarbanel, N.F. Rulkov, and M.M. Sushchik, Phys. Rev. E **53**, 4528 (1996).
 - [7] S.J. Schiff, P. So, T. Chang, R.E. Burke, and T. Sauer, Phys. Rev. E **54**, 6708 (1996).
 - [8] R. Quiñero, J. Arnhold, and P. Grassberger, Phys. Rev. E **61**, 5142 (2000).
 - [9] P.L. Lai and C. Fyfe, Int. J. of Neural Sys. **10**, 365 (2000); S. Akaho, In *Proceedings of the International Meeting of the Psychometric Society (IMPS2001)*, (Springer, Tokyo, 2001); F.R. Bach and M.I. Jordan, J. of Machine Learning Res. **3**, 1 (2002).
 - [10] J. Shawe-Taylor and N. Cristianini, *Kernel Methods for Pattern Recognition* (Cambridge University Press, Cambridge, 2004).
 - [11] K.-R. Müller et al., IEEE Trans. on Neural Networks **12**, 181 (2001).
 - [12] B. Schölkopf and A.J. Smola, *Learning with Kernels, Support Vector Machines, Regularization, Optimization,*

and Beyond (The MIT Press, Cambridge, 2002).

- [13] H. Hotelling, *Biometrika* **28**, 321 (1936).
- [14] Recently, statistical consistency of Kernel CCA, i.e., convergence of f, g to the optimal ones in a RKHS, is proved under the condition that $\kappa/N \sim N^{-1/3+\delta}$ ($0 < \delta < 1/3$) with $N \rightarrow \infty$. K. Fukumizu, F.R. Bach, and A. Gretton: Consistency of Kernel Canonical Correlation Analysis, ISM Research Memorandum No.942 (2005).
- [15] S.K. Han et al., *Int. J. Bifur. and Chaos* **12**, 983 (2002).
- [16] M.G. Rosenblum, A.S. Pikovsky, and J. Kurths, *Phys. Rev. Lett.* **76**, 1804 (1996).
- [17] M. Stone, *J. Roy. Statist. Soc. B* **36**, 111 (1974).
- [18] H. Suetani, Y. Iba, and K. Aihara, to be submitted.